Mathematical Modelling and Analysis
Volume 11 Number 4, 2006, pages 365–378
 ISSN 1392-6292 print, ISSN 1648-3510 online

ROBUST NUMERICAL METHODS FOR BOUNDARY-LAYER EQUATIONS FOR A MODEL PROBLEM OF FLOW OVER A SYMMETRIC CURVED SURFACE[1]

A.R. ANSARI[1], B. HOSSAIN[2], B. KOREN[3] and G.I. SHISHKIN[4]

[1] *Gulf University for Science & Technology*
Department of Mathematics & Natural Sciences, Hawally 32093, P.O. Box 7207, Kuwait
E-mail: ansari.a@gust.edu.kw

[2] *University of Limerick*
Department of Mathematics & Statistics, Limerick, Ireland
E-mail: bayezid.hossain@ul.ie

[3] *Delft University of Technology*
Faculty of Aerospace Engineering, Aerodynamics Group, P.O. Box 5058, 2600 GB Delft, The Netherlands
E-mail: B.Koren@LR.TUDelft.nl

[4] *Russian Academy of Sciences*
Institute of Mathematics and Mechanics, Ekaterinburg, Russia
E-mail: shishkin@imm.uran.ru

Received March 3, 2006; revised June 18, 2006; published online December 15, 2006

Abstract. We investigate the model problem of flow of a viscous incompressible fluid past a symmetric curved surface when the flow is parallel to its axis. This problem is known to exhibit boundary layers. Also the problem does not have solutions in closed form, it is modelled by boundary-layer equations. Using a self-similar approach based on a Blasius series expansion (up to three terms), the boundary-layer equations can be reduced to a Blasius-type problem consisting of a system of eight third-order ordinary differential equations on a semi-infinite interval. Numerical methods need to be employed to attain the solutions of these equations and their

[1] This work was supported in part by the Department of Mathematics, Gulf University for Science & Technology, by the Russian Foundation for Basic Research (grants Nos. 04-01-00578, 04-01-89007-NWO_a), by the Dutch Research Organisation NWO (grant No. 047.016.008) and by the Department of Mathematics & Statistics, University of Limerick.

derivatives, which are required for the computation of the velocity components, on a finite domain with accuracy independent of the viscosity ν, which can take arbitrary values from the interval $(0, 1]$. To construct a robust numerical method we reduce the original problem on a semi-infinite axis to a problem on the finite interval $[0, K]$, where $K = K(N) = \ln N$. Employing numerical experiments we justify that the constructed numerical method is parameter robust.

Key words: body of revolution, numerical methods, parameter robust, boundary layers

1. Introduction

In this paper we consider a model problem of viscous fluid flow past a body represented by a symmetric curved surface. The flow is taken parallel to the axis of the body, this gives rise to boundary layers on the surface of the body.

Some linear and nonlinear two-dimensional problems arising in the boundary-layer theory (see, *e.*g., [5, 6]) have been treated numerically using piecewise uniform meshes (see, *e.g.,* [1, 2, 3, 4, 7, 8] and the bibliography therein). For boundary layers on the curved body under study here we have to deal with more complicated geometries and singularities of the solution related to the stagnation point. Assuming a curvilinear coordinate system we denote the length along a meridian from the stagnation point by x, and the coordinate at right angles to the surface by y. The contour of the body of revolution is represented by radii $r(x)$, which essentially represents the sections taken at right angles to the axis of the body of revolution. We will assume that there are no sharp corners along the meridian (*i.e.,* $\dfrac{d^2r}{dx^2}$ is continuous) and, moreover, $\dfrac{d^2r}{dx^2}$ does not become large. We further assume that the minimum radius of curvature of the meridian arc for the body of revolution is much larger than the thickness of the boundary layer. Furthermore, we denote the velocity components as u parallel to the surface, and v normal to the surface. The potential flow is denoted by $U(x)$. The steady-state boundary-layer equations for this problem can be written as [6]

$$\begin{cases} u\dfrac{\partial u}{\partial x} + v\dfrac{\partial u}{\partial y} = -\dfrac{1}{\rho}\dfrac{\partial p}{\partial x} + \nu\dfrac{\partial^2 u}{\partial y^2}, \\ \dfrac{\partial (ur)}{\partial x} + \dfrac{\partial (vr)}{\partial y} = 0, \end{cases} \tag{1.1}$$

with the boundary conditions

$$u(x,0) = v(x,0) = 0, \quad \lim_{y\to\infty} u(x,y) = U(x), \tag{1.2}$$

where ρ is the density, ν is the viscosity of the fluid and p is the pressure. Standard magnitude analysis shows that the pressure gradient in the $y-$direction is approximately of order one [6]. It is now possible to assume that the pressure gradient of the potential flow velocity $U(x)$ is acting on the boundary layer in the following manner:

$$U\frac{dU}{dx} = -\frac{1}{\rho}\frac{\partial p}{\partial x}. \tag{1.3}$$

For the purpose of our analysis here we will consider the body contour to be defined by

$$r(x) = R\left\{\frac{x}{R} - \frac{1}{3!}\frac{x^3}{R^3} + \frac{1}{5!}\frac{x^5}{R^5}\right\}, \tag{1.4}$$

where r is the radius of the section of the surface. The velocity distribution at the surface of the body is given by

$$U(x) = \frac{3}{2}U_\infty\left\{\frac{x}{R} - \frac{1}{3!}\frac{x^3}{R^3} + \frac{1}{5!}\frac{x^5}{R^5}\right\}, \tag{1.5}$$

where U_∞ is the free-flow velocity parallel to the x-axis. In (1.4) and (1.5) $\frac{x}{R}$ denotes the central angle measured from the stagnation point. We emphasize that in this paper we study a computational method and not a flow problem. These days, for solving flow problems around geometries like described in Fig. 1, the full Navier-Stokes equations are to be preferred above the boundary-layer equations.

The simple geometry of the body given by (1.4) is chosen merely in order to demonstrate a computational method. This method turns out to be applicable in practice for bodies of revolution with more general contours for which the minimal radius of curvature of the meridian arc remains much larger than the thickness of the boundary layer arising in the flow problem in question.

It is known that as the viscosity ν of the fluid changes, the thickness of the boundary layer is affected. It is desirable to have numerical methods for which the associated errors for the velocity components u, v are independent of the viscosity ν. Although from a physical point of view ν may not approach zero, nevertheless we will consider the full range of its values $\nu \in (0, \nu_0]$, for some fixed ν_0, for the purpose of testing our method. A self-similar approach to generate the velocity components using a Blasius series expansion up to two terms, *i.e.,* a curved body with a parabolic profile is discussed in [3], where we solve a system of three ordinary differential equations numerically. The work that will follow in the succeeding sections concerns a self-similar approach to finding the velocity components using a Blasius series expansion up to three terms. Here a system of eight ordinary differential equations needs to be solved numerically. The approach here is similar to the approach introduced in [3] for the boundary layer on a body of revolution and to that in [2] for the boundary layer over a flat plate, respectively. However, only one ordinary differential equation was required in [2] and three ordinary differential equations were required to find the solution in [3]. Here the problem is more complicated as simultaneous numerical solution of eight ordinary differential equations is required. On the basis of the assumption (1.4), we draw the body profile including the third term. The body is an axially symmetric curved surface, see Fig. 1, where $R = 1$.

Our approach is build on the work of [3] but we solve the extra five differential equations. As we shall show in Section 4, the obtained results together

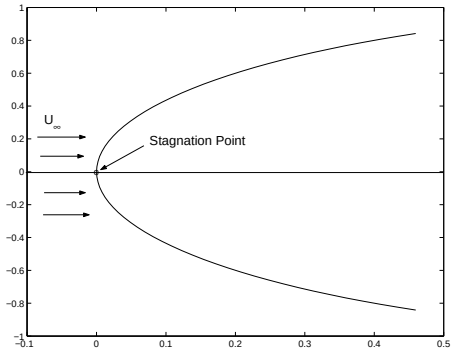

Figure 1. Body profile for $r(x) = x - \dfrac{x^3}{6R^2} + \dfrac{x^5}{120R^4}$.

with the results in [3] allow us to compute the velocity components. We will employ monotone methods similar to [2], [3] to find the self-similar solution of problem (1.1)–(1.5).

As noted in [6, Section 11], a Blasius series approach is applicable for bodies of revolution of any form, but it is most tedious. In this connection it is important to develop efficient *robust* numerical methods for implementation of this approach in practice.

The method suggested in this paper is indeed parameter robust, and it allows us to determine numerically the velocity components and their derivatives with controllable accuracy which is defined only by the number of mesh points used. Robust methods of this type are attractive to be applied to other problems with boundary layers whose solutions exhibit self-similar behaviour. The present paper shows the efficiency of the developed numerical method for the study and computation of the flow over symmetric curved surfaces in that case when the thickness of the boundary layer is small as compared to the radius of curvature of the meridian arc at each point of the streamlined body.

2. Problem Formulation

As mentioned in [3], it is worth noting that no explicit solutions are known for problem (1.1)–(1.5). Following the analysis of [6] employing a Blasius series approach, it is possible to attain a semi-analytical, self-similar solution $\mathbf{u}_B = (u_B, v_B)$ which can be written as

$$u_B(x,y) = \frac{\partial \psi}{\partial y}, \quad v_B(x,y) = -\frac{\partial \psi}{\partial x} - \frac{1}{r}\frac{dr}{dx}\psi, \tag{2.1}$$

where ψ is the flow function. Using (1.3), (2.1) reduces equation (1.1) to

$$\frac{\partial \psi}{\partial y}\frac{\partial^2 \psi}{\partial x \partial y} - \left(\frac{\partial \psi}{\partial x} + \frac{1}{r}\frac{dr}{dx}\psi\right)\frac{\partial^2 \psi}{\partial y^2} = U\frac{dU}{dx} + \nu\frac{\partial^3 \psi}{\partial y^3},$$

with the boundary conditions

$$\psi(x,0) = \frac{\partial \psi}{\partial y}(x,0) = 0, \quad \lim_{y\to\infty} \frac{\partial \psi(x,y)}{\partial y} = U(x).$$

In [3] we considered the case of a simple geometry with the first two terms of the Blasius series expansion. Here because of the geometry given by (1.4), our aim is to consider the Blasius series expansion with three terms, that leads to the flow function

$$\psi(x,y) = \sqrt{\frac{\nu U_\infty R}{12}} \left[3\frac{x}{R} f_1(\eta) - \left(\frac{x}{R}\right)^3 f_3(\eta) + \frac{1}{40}\left(\frac{x}{R}\right)^5 f_5(\eta) \right],$$

with

$$\eta = \frac{y}{R}\sqrt{\frac{3U_\infty R}{\nu}}. \tag{2.2}$$

We are interested in finding $\mathbf{u}_B$, *i.e.,* the self-similar solution of problem (1.1)–(1.5) in the rectangular domain $\bar{\Omega} = (0,1)\times(0,1)$. Thus, in accordance with (2.1) the velocity components are given by

$$\begin{cases} u_B(x,y) = \dfrac{3U_\infty}{2R} x f_1'(\eta) - \dfrac{U_\infty}{2R^3} x^3 f_3'(\eta) + \dfrac{3U_\infty}{80R^5} x^5 f_5'(\eta), \\ v_B(x,y) = -\sqrt{\dfrac{3\nu U_\infty}{R}} \left\{ v_{B_1}(x) f_1(\eta) - v_{B_2}(x) f_3(\eta) + v_{B_3}(x) f_5(\eta) \right\}, \end{cases} \tag{2.3}$$

where

$$v_{B_1}(x) = \frac{120R^4 - 40x^2R^2 + 3x^4}{120R^4 - 20x^2R^2 + x^4}, \quad v_{B_2}(x) = \left(\frac{80R^4 - 20x^2R^2 + \frac{4}{3}x^4}{120R^4 - 20x^2R^2 + x^4}\right)\frac{x^2}{R^2},$$

$$v_{B_3}(x) = \left(\frac{72R^4 - 16x^2R^2 + x^4}{120R^4 - 20x^2R^2 + x^4}\right)\frac{x^4}{8R^4} \tag{2.4}$$

and η is given by (2.2) and the viscosity ν can take arbitrary values in the half interval $(0,1]$. Thus, both components $u(x,y)$ and $v(x,y)$, $(x,y)\in\bar{\Omega}$ depend on the parameter ν. Here $f_1(\eta)$ is the solution of the problem

$$\begin{cases} f_1'''(\eta) = -f_1(\eta) f_1''(\eta) + \dfrac{1}{2}\left(f_1'^2(\eta) - 1\right), \quad 0 < \eta < \infty, \\ f_1(0) = f_1'(0) = 0, \quad \lim_{\eta\to\infty} f_1'(\eta) = 1. \end{cases} \tag{2.5}$$

The function $f_3(\eta)$ can be represented by the sum of two functions

$$f_3(\eta) = g_3(\eta) + h_3(\eta), \tag{2.6}$$

where the function $g_3(\eta)$ is the solution of the boundary–value problem

$$\begin{cases} g_3'''(\eta) = -f_1(\eta) g_3''(\eta) + 2f_1'(\eta) g_3'(\eta) - 2f_1''(\eta) g_3(\eta) - 1, \quad 0 < \eta < \infty, \\ g_3(0) = g_3'(0) = 0, \quad \lim_{\eta\to\infty} g_3'(\eta) = \dfrac{1}{2}, \end{cases} \tag{2.7}$$

and the function $h_3(\eta)$ is the solution of the boundary–value problem

$$\begin{cases} h_3'''(\eta) = -f_1(\eta)h_3''(\eta) + 2f_1'(\eta)h_3'(\eta) - 2f_1''(\eta)h_3(\eta) - \frac{1}{2}f_1(\eta)f_1''(\eta), \\ h_3(0) = h_3'(0) = 0, \quad \lim_{\eta\to\infty} h_3'(\eta) = 0, \quad 0 < \eta < \infty. \end{cases} \tag{2.8}$$

The function $f_5(\eta)$ can be represented by the sum of five functions

$$f_5(\eta) = g_5(\eta) + h_5(\eta) + \frac{10}{3}k_5(\eta) + \frac{10}{3}j_5(\eta) + \frac{10}{3}q_5(\eta), \tag{2.9}$$

where the functions $g_5(\eta)$, $h_5(\eta)$, $k_5(\eta)$, $j_5(\eta)$, and $q_5(\eta)$ are solutions of the following boundary-value problems

$$\begin{cases} g_5'''(\eta) = -f_1(\eta)g_5''(\eta) + 3f_1'(\eta)g_5'(\eta) - 3f_1''(\eta)g_5(\eta) - 1, \\ g_5(0) = g_5'(0) = 0, \quad \lim_{\eta\to\infty} g_5'(\eta) = \dfrac{1}{3}, \quad 0 < \eta < \infty; \end{cases} \tag{2.10}$$

$$\begin{cases} h_5'''(\eta) = -f_1(\eta)h_5''(\eta) + 3f_1'(\eta)h_5'(\eta) - 3f_1''(\eta)h_5(\eta) - \frac{2}{3}f_1(\eta)f_1''(\eta), \\ h_5(0) = h_5'(0) = 0, \quad \lim_{\eta\to\infty} h_5'(\eta) = 0, \quad 0 < \eta < \infty; \end{cases} \tag{2.11}$$

$$\begin{cases} k_5'''(\eta) = -f_1(\eta)k_5''(\eta) + 3f_1'(\eta)k_5'(\eta) - 3f_1''(\eta)k_5(\eta) \\ \qquad -2g_3'^2(\eta) - \frac{8}{3}g_3g_3'' - \frac{1}{2}, \\ k_5(0) = k_5'(0) = 0, \quad \lim_{\eta\to\infty} k_5'(\eta) = 0, \quad 0 < \eta < \infty; \end{cases} \tag{2.12}$$

$$\begin{cases} j_5'''(\eta) = -f_1(\eta)j_5''(\eta) + 3f_1'(\eta)j_5'(\eta) - 3f_1''(\eta)j_5(\eta) + 4\,g_3'(\eta)h_3'(\eta) \\ \qquad -\frac{8}{3}\,(g_3\,h_3'' + h_3\,g_3'') - \frac{2}{3}\,(f_1''\,g_3 + f_1 g_3''), \quad 0 < \eta < \infty, \\ j_5(0) = j_5'(0) = 0, \quad \lim_{\eta\to\infty} j_5'(\eta) = 0; \end{cases} \tag{2.13}$$

$$\begin{cases} q_5'''(\eta) = -f_1(\eta)q_5''(\eta) + 3f_1'(\eta)q_5'(\eta) - 3f_1''(\eta)q_5(\eta) + 2h_3'^2 \\ \qquad -\frac{8}{3}h_3h_3'' + \frac{1}{3}f_1f_1'' - \frac{2}{3}(f_1h_3'' + f_1''h_3), \quad 0 < \eta < \infty, \\ q_5(0) = q_5'(0) = 0, \quad \lim_{\eta\to\infty} q_5'(\eta) = 0. \end{cases} \tag{2.14}$$

As mentioned earlier, the system (2.5)–(2.8) has already been solved numerically (see [3]), here our aim is to construct a robust numerical method for the singular system (2.5)–(2.14), *i.e.*, a method for which the accuracy of the components $u_B(x,y)$ and $v_B(x,y)$ given by (2.3)–(2.4), respectively, is independent of the parameter ν, and is defined only by the number of mesh points used to solve problem (2.5)–(2.14) on $[0,\infty)$. To construct such a robust method in accordance with (2.3)–(2.4), it is sufficient to have an

accurate method to approximate $f_1(\eta), f_3(\eta)$ (or $g_3(\eta), h_3(\eta)$) and $f_5(\eta)$, (or $g_5(\eta), h_5(\eta), k_5(\eta), j_5(\eta), q_5(\eta)$) and all respective first derivatives uniformly on the semi-infinite axis $[0, \infty)$.

Note that when the parameter ν is bounded from below, *i.e.,* $\nu \geq \nu_0 > 0$, then η varies on the bounded interval $[0, \eta_0]$, for all $(x, y) \in \bar{\Omega}$, where

$$\eta_0 = \frac{1}{R}\sqrt{\frac{3U_\infty R}{\nu_0}}.$$

It is worth noting that the computation of the components $u_B(x, y)$ and $v_B(x, y)$ for $(x, y) \in \bar{\Omega}$, $\nu \in [\nu_0, 1]$, if $f_1'(\eta_0)$, $g_3'(\eta_0)$, $h_3'(\eta_0)$, $g_5'(\eta_0)$, $h_5'(\eta_0)$, $k_5'(\eta_0)$, $j_5'(\eta_0)$ and $q_5'(\eta_0)$ are given, is a simple problem, *i.e.,* no specific robust method is required.

3. The Numerical Solution

In the succeeding subsections we first construct numerical methods to solve problems (2.10)–(2.14), which give us the approximations to g_5, h_5, k_5, j_5 and q_5, respectively, which in turn give us f_5. For brevity we outline the principles of our numerical methods and then we demonstrate explicitly our constructed numerical method by solving problem (2.10). Finally, using these numerical solutions *i.e.*, the numerical approximations of f_1, f_3 and f_5 we compute the required velocity components. In section 4, we will show with the aid of numerical experiments that the constructed numerical method is robust.

The equations and boundary conditions for problems (2.10)–(2.14) have been defined in Section 2. All the equations are linear. As discussed in [2] and [3], instead of solving problems (2.10)–(2.14) on a semi-infinite domain $[0, \infty)$ we solve them on a finite domain $[0, K]$, for an increasing sequence of values of the length K, where K is an auxiliary parameter. To determine approximate solutions on the domain $[K, \infty)$, we extend the function, *e.g.*, F_K, by using the following extrapolations

$$F_K''(\eta) = 0, \quad F_K'(\eta) = L, \quad \forall \eta \geq K \tag{3.1}$$

$$F_K(\eta) = L\,(\eta - K) + F_K(K), \quad \forall \eta \geq K, \tag{3.2}$$

where (3.2) can be obtained by integrating both sides of (3.1) from K to η and L is the limiting value of the first derivative of any function F.

To solve problems (2.10)–(2.14) we use a finite-difference approximation on a uniform mesh on the interval $[0, K_N]$ with N mesh nodes [2]

$$\bar{I}^N = \{\eta_i \mid \ \eta_i = iN^{-1}K_N, \ \ 0 \leq i \leq N\}, \tag{3.3}$$

where $K_N = \ln N$ and we compute numerical approximations F, D^+F and D^+D^+F to f_K, f_K' and f_K'' respectively, at the mesh points $\bar{I}^N$ using the linear finite-difference method:

$$(S_B^N)\quad \begin{cases} \text{Find } F \text{ such that } \forall \eta_i \in I^N \\ \delta^2(D^-F)(\eta_i) + F_1(\eta_i)D^+(D^-F)(\eta_i) - C\,(D^+F_1)(\eta_i)(D^-F)(\eta_i) \\ \qquad\qquad +C\,D^-(D^+F_1)(\eta_i)F(\eta_i) = R_i \\ F(0) = D^+F(0) = 0, \quad D^0F(\eta_{N-1}) = L, \end{cases}$$

where C is a constant, R_i is the righthand side, which depends on previously determined functions *e.g.*, f_1, g_3, h_3 and so on.

It is worth mentioning that the use of the backward finite-difference D^-F in the finite-difference scheme $\left(S_B^N\right)$ ensures that this numerical method is monotone, its solution exists and is unique with the given boundary conditions [2]. Further, we mention that the use of the centered finite-difference operator D^0, which is a higher-order approximation of the first derivative [2], in the righthand boundary condition also ensures the monotonicity of the numerical method.

3.1. Numerical solution of problem (2.10)

The equations and boundary conditions for problems (2.10)–(2.14) have been defined in Section 2. As mentioned earlier, we proceed by solving problem (2.10) on a finite domain $[0, K]$, where K is an auxiliary parameter. Thus we can express (2.10) as

$$\begin{cases} g'''_{5_K}(\eta) + f_{1_K}(\eta)g''_{5_K}(\eta) - 3f'_{1_K}(\eta)g'_{5_K}(\eta) + 3f''_{1_K}(\eta)g_{5_K}(\eta) = -1, \\ g_{5_K}(0) = g'_{5_K}(0) = 0, \quad g'_{5_K}(K) = \dfrac{1}{3}. \end{cases} \tag{3.4}$$

To determine approximate solutions on the domain $[K, \infty)$, we extend the function g_{5_K} by using the extrapolation

$$g_{5_K}(\eta) = \frac{1}{3}(\eta - K) + g_{5_K}(K), \quad \forall \eta \geq K. \tag{3.5}$$

And from (3.5), we have

$$g'_{5_K}(\eta) = \frac{1}{3}, \quad g''_{5_K}(\eta) = 0, \quad \forall \eta \geq K. \tag{3.6}$$

Thus, the auxiliary problems (3.4)–(3.6) for given $f_{1_K}(\eta)$, $f'_{1_K}(\eta)$, $f''_{1_K}(\eta)$ are defined by the parameter K. The solution $g_5(\eta)$ of the problem (2.10) is the limiting solution of the problem (3.4)–(3.6) for $K \to \infty$. Considerations similar to those given in [2] for flow over a flat plate (see Chapter 11, Section 3) lead to the relation

$$\left| g'_5(\eta) - \frac{1}{3} \right| \approx M \exp(-\frac{1}{2}\eta^2),$$

for sufficiently large η. The boundary condition for $g'_{5_K}(K)$ in (3.4) is obtained taking into account the behaviour of the derivative $g'_5(\eta)$ for large values of η.

To solve problem (3.4) we use a finite-difference approximation on the uniform mesh (3.3) on the interval $[0, K_N]$ with N number of mesh nodes [2]. Problem (3.4) is approximated by the following finite-difference scheme

$$\begin{cases} \delta^2(D^-G_5)(\eta_i) + F_{1_K}(\eta_i)D^+(D^-G_5)(\eta_i) - 3(D^+F_{1_K})(\eta_i) \\ \qquad \times(D^-G_5)(\eta_i) + 3D^-(D^+F_{1_K})(\eta_i)G_5(\eta_i) = -1, \\ G_5(0) = D^+G_5(0) = 0, \quad D^0G_5(\eta_{N-1}) = \dfrac{1}{3}, \end{cases} \tag{3.7}$$

where

$$D^-G_5(\eta_i) \equiv \frac{G_5(\eta_i) - G_5(\eta_{i-1})}{h}, \quad D^+G_5(\eta_i) \equiv \frac{G_5(\eta_{i+1}) - G_5(\eta_i)}{h},$$
$$\delta^2G_5(\eta_i) \equiv \frac{D^+G_5(\eta_i) - D^-G_5(\eta_i)}{h}, \quad D^0G_5(\eta_i) \equiv \frac{G_5(\eta_{i+1}) - G_5(\eta_{i-1})}{2h}$$

and the mesh spacing is defined as $h = \dfrac{K_N}{N}$.

The discrete function $F_{1_K}(\eta_i)$ is an approximation of the function $f_1(\eta)$, which is the solution of problem (2.5) (see [3]). For $\eta \in [K_N, \infty)$, we use

$$\overline{G}_{5_K}(\eta_i) = \frac{1}{3}(\eta_i - K_N) + \overline{G}_{5_K}(K_N), \quad \forall \eta \geq K_N. \tag{3.8}$$

The solution of the problem (3.7)–(3.8) depends on two parameters K and N. Similar to [2], one can justify that under the condition

$$K_N = \ln N, \tag{3.9}$$

the solution G_5, *i.e.,* solution of the problem (3.7)–(3.9) depends on the parameter N only and converges to the function $g_5(\eta)$ uniformly on $[0, \infty)$ (we use here the technique similar to that given in [2, Chapter 11, Section 6]). Employing the above mentioned principles of the constructed numerical method we solve problems (2.10), (2.11), (2.12), (2.13) and (2.14) jointly with (2.5).

4. Numerical Experiments

In this section we present the results of computations performed using the numerical method outlined in the previous section. To proceed to the error analysis we first introduce some notions related to the errors and orders of convergence that we will employ here. For any mesh function W^N on $\bar{I}^N$, we denote by W^{N^*}, the numerical solution on the finest mesh $\bar{I}^{N^*}$, which here corresponds to $N^* = 32768$, and by $\overline{W}^{N^*}$ we define its piecewise linear interpolant. We take $\overline{W}^{N^*}$ as the reference solution. We define the maximum pointwise errors

$$F^N = \max_{\bar{I}^N} \|W^N - \overline{W}^{N^*}\|_\infty. \tag{4.1}$$

We also analyze the errors in the numerical solutions in a different way, which does not depend on *a priori* knowledge of the exact solution. We introduce the computed pointwise two-mesh differences

$$D^N = \max_{\bar{I}^N} \|W^N - \overline{W}^{2N}\|_\infty, \tag{4.2}$$

which is the difference between any two consecutive meshes. We also define the orders of convergence $R^N = \log_2(D^N/D^{2N})$, which are based on the two mesh differences.

We introduce the computed global two-mesh differences $\overline{D}^N$, which have to be computed over three sub-intervals $[0, K_N)$, $[K_N, K_{2N})$ and $[K_{2N}, \infty)$ separately.

For $\eta \in [0, K_N)$, the two-mesh difference for $\overline{W}$ is $\max_{[0,K_N]} \|\overline{W}^N - \overline{W}^{2N}\|$ and for $\overline{D^+W}$ it is $\max_{[0,K_N]} \|\overline{D^+W}^N - D^+W^{2N}\|$. For $\eta \in [K_N, K_{2N})$, the two-mesh difference at η for $\overline{W}$ is $\max_{[K_N,K_{2N}]} \|\overline{W^{2N}}(\eta) - W^N(K_N) - L(\eta - K_N)\|$ and for $\overline{D^+W}$ is $\|\overline{D^+W^{2N}} - L\|$. We consider $L = \frac{1}{3}$ for f_5. Note that $K_{2N} = \ln 2N$. The two-mesh difference in the sub-interval $[K_{2N}, \infty)$ at η for $\overline{W}$ is $\|W^{2N}(K_{2N}) - W^N(K_N) - L \ln 2\|$ and for $\overline{D^+W}$ it is zero. In this manner we compute the global two mesh differences $\bar{D}^N$ over $[0, \infty]$ for various values of N. We finally define the orders of convergence $\bar{R}^N = \log_2(\bar{D}^N/\bar{D}^{2N})$, which are based on the computed global two mesh differences.

We will now compute E^N, D^N, R^N, $\bar{D}^N$ and $\bar{R}^N$ for the numerical solution of the problem for f_5 in the following subsections.

4.1. Computed solution and error analysis for f_5

A graph of the function $\overline{F}_5(\eta)$ for $N = 8192$ on $[0, K_N]$ is given in Fig. 2. Here in comparison to f_1 and f_3 (computed in [3]), we note that the function f_5 shows non-monotonic behaviour. This is clearly seen from Fig. 2 (see parts (a) and (b)). The results given in Table 1 correspond to the solution F_5.

Table 1. Maximum pointwise errors F^N, computed two-mesh differences D^N and computed orders of convergence R^N for F_5 for various values of N.

N	128	256	512	1024	2048	4096	8192	16392
F^N	1.980D-02	1.110D-02	6.273D-03	3.447D-03	1.831D-03	9.247D-04	4.237D-04	1.495D-04
D^N	9.575D-03	4.822D-03	2.826D-03	1.616D-03	9.062D-04	5.010D-04	2.741D-04	1.495D-04
R^N	0.99	0.77	0.81	0.83	0.86	0.87	0.87	

In Tables 2 and 3 the results for approximation of the derivatives D^+F_5 and $D^+D^+F_5$ are given, respectively.

We note that all tables reflect a uniform convergence on $\bar{I}^N$. The order of uniform convergence of the numerical solution F_5 to the exact solution f_{5_K}

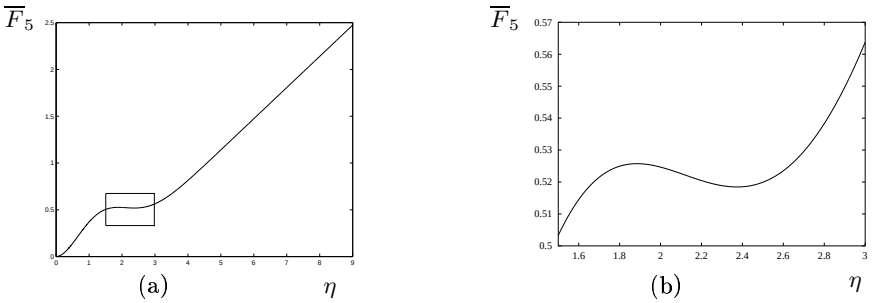

Figure 2. (a) A plot of the solution of $\overline{F}_5$ for $N = 8192$, (b) a zoomed boxed area.

Table 2. Maximum pointwise errors F^N, computed two-mesh differences D^N and computed orders of convergence R^N for D^+F_5 for various values of N.

N	128	256	512	1024	2048	4096	8192	16392
F^N	2.700D-02	1.556D-02	8.750D-03	4.790D-03	2.538D-03	2.280D-03	5.855D-04	2.060D-04
D^N	1.145D-02	6.809D-03	3.959D-03	2.251D-03	1.258D-03	6.943D-04	3.795D-04	2.060D-04
R^N	0.75	0.78	0.81	0.84	0.86	0.87	0.88	

Table 3. Maximum pointwise errors F^N, computed two-mesh differences D^N and computed orders of convergence R^N for $D^+D^+F_5$ for various values of N.

N	128	256	512	1024	2048	4096	8192	16392
F^N	9.295D-02	5.271D-02	2.926D-02	1.589D-02	8.380D-03	4.214D-03	1.924D-03	6.760D-04
D^N	4.023D-02	2.345D-02	1.337D-02	7.508D-03	4.166D-03	2.290D-03	1.249D-03	6.760D-04
R^N	0.78	0.81	0.83	0.85	0.86	0.88	0.89	

on $[0, K_N]$ is better than 0.8 for all $N \geq 512$. We observe similar orders of convergence of the discrete derivative D^+F_5 to the derivative f'_{5_K} for $N \geq 512$ on $[0, K_N]$. The orders of convergence of the discrete derivative $D^+D^+F_5$ to the derivative f''_{5_K} on $[0, K_N]$ are better than 0.8 for all $N \geq 256$.

It can also be observed that the maximum point-wise error F^N and the convergence rate of the computed two-mesh difference D^N of the numerical solution F_5 and of the discrete derivatives D^+F_5 and $D^+D^+F_5$ to the exact solution f_{5_K} and to the derivatives f'_{5_K} and f''_{5_K} respectively, on $[0, K_N]$ reflect the uniform convergent behaviour. In other words notice the trend in columns labeled E^N and D^N in Tables 1, 2 and 3, where the errors are reducing as N increases.

The global two mesh differences given in Table 4 correspond to the function $\overline{F}_5$, and in Tables 5 and 6 the global two mesh differences correspond to the derivatives $\overline{D^+F_5}$ and $\overline{D^+D^+F_5}$, respectively. Function $\overline{F}_5$ and derivatives $\overline{D^+F_5}$ and $\overline{D^+D^+F_5}$ are convergent uniformly on $[0, \infty)$ and the computed global orders of convergence for $\overline{F}_5$ are better than 0.8 for all $N \geq 512$. We

Table 4. Computed two-mesh differences $\bar{D}^N$ and computed orders of convergence $\bar{R}^N$ for $\overline{F}_5$ on $[0,\infty)$ for various values of N.

N	128	256	512	1024	2048	4096	8192	16392
$\bar{D}^N$	9.533D-03	4.833D-03	2.829D-03	1.617D-03	9.065D-04	5.011D-04	2.742D-04	1.495D-04
$\bar{R}^N$	0.98	0.77	0.81	0.83	0.86	0.87	0.87	

observe similar orders of convergence of the derivative $\overline{D^+F_5}$ for $N \geq 512$. In addition, the orders of convergence of the derivative $\overline{D^+D^+F_5}$ are better than 0.8 for all $N \geq 256$.

Table 5. Computed two-mesh differences $\bar{D}^N$ and computed orders of convergence $\bar{R}^N$ for $\overline{D^+F_5}$ on $[0,\infty)$ for various values of N.

N	128	256	512	1024	2048	4096	8192	16392
$\bar{D}^N$	1.157D-02	6.849D-03	3.974D-03	2.255D-03	1.260D-03	6.947D-04	3.796D-04	2.060D-04
$\bar{R}^N$	0.77	0.79	0.82	0.84	0.86	0.87	0.88	

Table 6. Computed two-mesh differences $\bar{D}^N$ and computed orders of convergence $\bar{R}^N$ for $\overline{D^+D^+F_5}$ on $[0,\infty)$ for various values of N.

N	128	256	512	1024	2048	4096	8192	16392
$\bar{D}^N$	4.023D-02	2.345D-02	1.337D-02	7.508D-03	4.166D-03	2.290D-03	1.249D-03	6.760D-04
$\bar{R}^N$	0.78	0.81	0.83	0.85	0.86	0.88	0.89	

Thus, the numerical approximations $\overline{F}_5$, $\overline{D^+F_5}$ and $\overline{D^+D^+F_5}$ are robust, *i.e.,* their accuracy in the maximum norm depends only on the value of N. Moreover, for increasing N the orders of their convergence are better than 0.8 for $N \geq 512$.

4.2. Computation of the semi–analytical solution

The computation of the self-similar semi-analytic solution $\mathbf{u}_B$ is now carried out using the numerical approximations $\overline{F}_5$ and $\overline{F}_5' = \overline{D^+F_5}$, which are substituted for the exact solution f_5 and for the discrete derivative f_5', respectively. In an analogous way $\overline{F}_1$, $\overline{F}_1' = \overline{D^+F_1}$, $\overline{F}_3$ and $\overline{F}_3' = \overline{D^+F_3}$ are substituted (see [3]) for f_1, f_1', f_3 and f_3', respectively. The relations (2.1) are used for each (x,y) in the rectangular domain $\bar{\Omega} = [0,1] \times [0,1]$. We define

$$U_B(x,y) = \frac{3U_\infty}{2R} x\, \overline{F}_1'(\eta) - \frac{U_\infty}{2R^3} x^3\, \overline{F}_3'(\eta) + \frac{3U_\infty}{80R^5} x^5\, \overline{F}_5'(\eta),$$

$$V_B(x,y) = -\sqrt{\frac{3\nu U_\infty}{R}} \left\{ v_{B_1}(x)\, \overline{F}_1(\eta) - v_{B_2}(x)\, \overline{F}_3(\eta) + v_{B_3}(x)\, \overline{F}_5(\eta) \right\},$$

where (2.4) represents $v_{B_1}(x)$, $v_{B_2}(x)$, $v_{B_3}(x)$ and $\eta = (0, \infty)$ is given by (2.2).

Graphs of the resulting approximate solution $\mathbf{u}_B$ are given in Figure 3 for $\nu = 2^{-5}$. Note that we set $U_\infty = 1$ and $R = 1$ for the computations. These graphs are constructed using the data of the Blasius solution for $\overline{F}_1$, $\overline{F}_3$ and $\overline{F}_5$ corresponding to $N = 8192$.

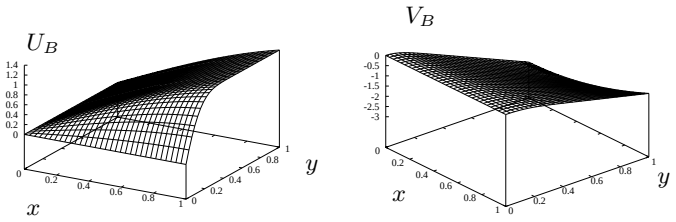

Figure 3. Graphs of the semi-analytical solution (U_B, V_B) for $\nu = 2^{-5}$ generated from the numerical solutions $\overline{F}_1$, $\overline{F}_3$ & $\overline{F}_5$. Graphs are given for a 32×32 mesh.

Having the robust approximations $\overline{F}_1$, $\overline{F}_3$, $\overline{F}_5$ and their discrete derivatives up to second order, one can compute the components $U_B(x, y)$, $V_B(x, y)$ and their first derivatives in x and y that are also parameter robust (see [2, Chapter 11, Section 7] for flow over a flat plate).

5. Conclusions

The aim of this work was to construct a robust numerical method to obtain a semi-analytical solution for the problems (1.1)–(1.3), (1.4), (1.5) over the symmetric curved surface on the domain $\bar{\Omega}$ based on the approach given in [6]. The body contour of the surface defined by (1.4), with associated velocity distribution on the surface defined by (1.5), results in the model flow on the surface being represented in terms of the functions f_1, f_3 and f_5, which are defined on the semi-axis $[0, \infty)$. To obtain a robust method for the velocity components u_B and v_B on the domain $\bar{\Omega}$ it is sufficient to have an accurate method to approximate f_1, f_3 and f_5 with their respective first derivatives, which are convergent uniformly on the semi-infinite axis $[0, \infty)$. In [3], we have considered a similar problem where the surface contour is represented by a third order polynomial, resulting in the model flow being represented by the functions f_1 and f_3, which involves a system of three ordinary differential equations. Using a similar approach we have constructed a robust numerical method to obtain a semi-analytical solution for the problem (1.1)–(1.3), (1.4), (1.5) on the domain $\bar{\Omega}$.

In this paper, we solve a system involving eight ordinary differential equations. In particular, we solve a system of five complicated auxiliary equations

to find g_5, h_5, k_5, j_5 and q_5 which generate f_5. Here the surface geometry is more complicated as the contour of the surface is represented by a 5th order polynomial. We note that in comparison to f_1 and f_3, the solution for f_5 shows non-monotonic behaviour, however, the discrete solution F_5 and its discrete derivatives D^+F_5 and $D^+D^+F_5$ reflect uniform convergent behaviour on $[0,\infty)$. The results we achieved here are not only the immediate extension of [3], we have indeed shown here that the constructed robust numerical method is applicable to more complicated surfaces for model problems in comparison to the body studied in [3].

The authors would like to thank the referee for some valuable comments on this paper.

References

[1] A.R. Ansari, A.F. Hegarty and G.I. Shishkin. A note on fitted operator methods for a laminar jet problem. *Appl. Numer. Math.*, **45**(4), 353–365, 2003.

[2] P.A. Farrell, A.F. Hegarty, J.J.H. Miller, E. O'Riordan and G.I. Shishkin. *Robust Computational Techniques for Boundary Layers.* Chapman & Hall/CRC Press, Boca Raton,, 2000.

[3] B. Hossain, A.R. Ansari and G.I. Shishkin. On numerical methods for a boundary layer on a body of revolution. *Comput. Methods Appl. Math.*, **3**(3), 405–416, 2003.

[4] J.J.H. Miller, E. O'Riordan and G.I. Shishkin. *Fitted Numerical Methods for Singular Perturbation Problems.* World Scientific, London, 1996.

[5] O.A. Oleinik and V.N. Samokhin. *Mathematical Models in Boundary-Layer Theory.* Chapman & Hall/CRC Press, Boca Raton, 1999.

[6] H. Schlichting. *Boundary-Layer Theory, 7th ed.* McGraw Hill, New York, 1979.

[7] G.I. Shishkin. A difference scheme on a non-uniform mesh for a differential equation with a small parameter in the highest derivative. *U.S.S.R. Compt. Maths. Math. Physics*, **23**, 59–66, 1983.

[8] G.I. Shishkin. *Discrete Approximations of Singular Perturbed Elliptic and Parabolic Equations.* Russian Academy of Sciences, Ural Section, Ekaterinburg, 1992. (in Russian)